A NEW APPROACH TO THE TRANSPORT OF HEAVY CHARGED PARTICLES

E.A. Youssef, F.E. Vermeulen and F.S. Chute

Department of Electrical Engineering, University of Alberta, Edmonton, Canada.

1. Summary

A study has been made of the focusing and guiding properties of a long electrostatic quadrupole structure that has been uniformly twisted about its axis. It is demonstrated that compared to the classical chain of quadrupole triplets, the twisted structure is inherently more strongly focusing and can accept more widely divergent particle beams.

2. Introduction

It is well established[1] that a chain of electrostatic quadrupole sections, separated by drift spaces, can provide a net focusing action when the electrode potentials are arranged so that a particle travelling along the structure is acted upon alternately by focusing and defocusing forces. This paper summarizes the transport properties of an analogous electrostatic system consisting of a single continuous electrostatic quadrupole section that has been uniformly twisted about its axis at a rate of β radians per unit length. Analytic expressions are obtained for particle trajectories along this structure and a particle confinement criterion is established. From this criterion analytic curves are derived that specify the acceptable limits of the initial transverse displacement and transverse momentum of a particle that is to be confined within the structure. A prototype of the structure is shown in Fig. 1. The electrodes, which are truncated hyperbolic sections, were moulded individually of epoxy resin and coated with conductive silver paint. This system has successfully guided particles with charge-to-mass ratios as low as 0.1 coulombs per Kgm.

A detailed evaluation is made of the acceptance of the twisted structure relative to that of the classical chain of quadrupole sections, for several special cases of injection. For purposes of comparison the quadrupole chain is assumed to be a cascade of symmetric triplets. Each triplet, as illustrated schematically in Fig. 2, consists of a straight quadrupole section of length, $\ell/2$, followed by a drift space of length, d, and a second straight section of length, ℓ. In this section the polarity of the electrodes has been reversed with respect to the potentials on the first quadrupole section. The second quadrupole element is followed by another drift space of length, d, and a third straight section which is identical to the first section. Both the twisted and classical structures are assumed to have the same aperture radius, a, and the same electrode potentials, $\pm V_o$. The classical channel has two complete triplets in the same axial length, L, as one complete turn of the twisted structure. Thus, from Fig. 2,

$$L = 4(\ell + d) \tag{1}$$

For both systems the polarity of electrodes will be taken such that the forces exerted on a charged particle are initially focusing in the X-Z plane and initially defocusing in the Y-Z plane.

3. Analysis of the Twisted Structure

The trajectories of particles along the twisted structure are most easily obtained by formulating the Hamiltonian of the motion in a rotating coordinate system (x,y,z) whose x,y axes are fixed with respect to the twisting electrodes[2]. When the rate of twist is small such that,

$$(\beta a)^2 = (2\pi a/L)^2 \ll 1, \tag{2}$$

the Hamiltonian, for a particle of mass m and charge q, may be expressed as

$$H = (1/2m)[p_x^2+p_y^2+p_z^2-2\beta p_z(xp_y-yp_x)]+ qV_o(x^2-y^2)/a^2 \tag{3}$$

where (p_x,p_y,p_z) are the momenta adjoint to (x,y,z). In the analysis to follow, β will be taken as a positive number representing rotation of the electrodes in a counterclockwise sense. The equations of motion thus become:

$$\begin{aligned}
\dot{p}_x &= (1/m)[\beta p_z p_y - (2qm\ V_o/a^2)x] \\
\dot{p}_y &= (1/m)[-\beta p_z p_x + (2qm\ V_o/a^2)y] \\
\dot{x} &= (1/m)[p_x + \beta p_z y] \\
\dot{y} &= (1/m)[p_y - \beta p_z x] \\
\dot{Z} &= \sqrt{2qV/m}
\end{aligned} \tag{4}$$

where the dot notation represents differentiation with respect to time and where V is the potential through which it is assumed that all particles have been accelerated prior to injection into the structure. Since from equation (3) it is apparent that p_z is a constant of the motion, equations (4) can be solved for (x,y,z,p_x and p_y)[3]. By a simple rotation of coordinates this solution may be expressed in terms of the fixed (X,Y,Z) coordinate system as:

$$\begin{bmatrix} X \\ Y \\ X' \\ Y' \end{bmatrix} = [R]\cdot[Q]\cdot \begin{bmatrix} X_o \\ Y_o \\ X'_o \\ Y'_o \end{bmatrix} \tag{5}$$

where

$$[R] = \text{rotational matrix} = \begin{bmatrix} \cos\beta z & -\sin\beta z & 0 & 0 \\ \sin\beta z & \cos\beta z & 0 & 0 \\ 0 & 0 & \cos\beta z & -\sin\beta z \\ 0 & 0 & \sin\beta z & \cos\beta z \end{bmatrix} \tag{6}$$

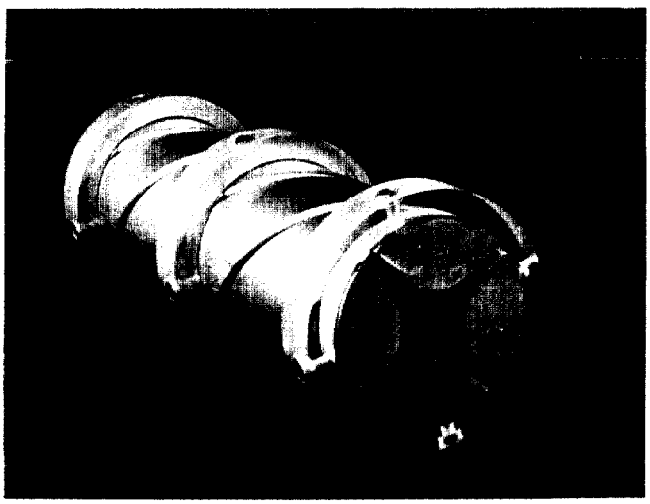

Fig. 1 A Prototype Section of the Twisted Structure.

$$[Q] = \begin{bmatrix} \cos\tau_1 z & -\sqrt{\frac{s}{s-1}}\sin\tau_2 z & \frac{\sqrt{s+1}}{\gamma}\sin\tau_1 z - \frac{s}{\gamma\sqrt{s-1}}\sin\tau_2 z & \frac{\sqrt{s}}{\gamma}(\cos\tau_2 z - \cos\tau_1 z) \\ -\sqrt{\frac{s}{s+1}}\sin\tau_1 z & \cos\tau_2 z & \frac{\sqrt{s}}{\gamma}(\cos\tau_1 z - \cos\tau_2 z) & \frac{s}{\gamma\sqrt{s+1}}\sin\tau_1 z - \sqrt{\frac{s-1}{\gamma}}\sin\tau_2 z \\ -\frac{\gamma}{\sqrt{s+1}}\sin\tau_1 z & 0 & \cos\tau_1 z & \sqrt{\frac{s}{s+1}}\sin\tau_1 z \\ 0 & \frac{\gamma}{\sqrt{s-1}}\sin\tau_2 z & -\sqrt{\frac{s}{s-1}}\sin\tau_2 z & \cos\tau_2 z \end{bmatrix} \quad (7)$$

X, Y = displacement of the particle in the X-direction and Y-direction at axial distance Z.

X_o, Y_o = initial values of X,Y at Z = 0.

$X' = P_X/P_Z$, $X'_o = P_{X_o}/P_{Z_o}$

$Y' = P_Y/P_Z$, $Y'_o = P_{Y_o}/P_{Z_o}$

P_X, P_Y, P_Z = momenta of the particle in the X, Y and Z directions at axial distance Z.

P_{X_o}, P_{Y_o}, P_{Z_o} = initial values of P_X, P_Y, P_Z at Z = 0.

$\tau_1 = \gamma\sqrt{s+1}$

$\tau_2 = \gamma\sqrt{s-1}$

$\gamma = \sqrt{V_o/V}/a$

$s = \beta^2 p^2/\gamma^2$

$p = 1 + \beta(X_o Y'_o - Y_o X'_o)$

The preceding representation which predicts stable motion along the twisted structure is valid only when the parameter s is such that $s > 1$. For the special cases of injection to be considered in this paper $p = 1$, and the above inequality may be expressed as

$$0 < \ell\sqrt{V_o/V}/4a < \pi/2 \quad (8)$$

The trajectories given by equations (6) can be interpreted in terms of cosine-like and sine-like modes of four fundamental spatial frequencies

$$\begin{aligned} \omega_1 &= [\sqrt{(s+1)/s} - 1]\beta \\ \omega_2 &= [1 - \sqrt{(s-1)/s}]\beta \\ \omega_3 &= [\sqrt{(s+1)/s} + 1]\beta \\ \omega_4 &= [1 + \sqrt{(s-1)/s}]\beta \end{aligned} \quad (9)$$

It is found that in general a typical particle trajectory features a dominant oscillation with an apparent wavelength of approximately four times the periodic length of the structure. Superimposed upon this oscillation appears a small ripple with an apparent wavelength approximately equal to half the periodic length. Some of the trajectories display a slow amplitude modulation over a length many times greater than the periodic length.

As a result of the coupling in the X and Y directions, values of X_{max} and Y_{max} cannot be specified independently. Rather, to ensure that a particle is confined within the quadrupole it is necessary that the total radial displacement be at most equal to the aperture radius. Thus,

$$r_{max} \leq a \ ,$$

or

$$(X^2 + Y^2)^{1/2} \leq a \quad (10)$$

From equations (6) it can be shown that the inequality (10) leads to a confinement criterion of the form:

$$\left|\left[\left(X_o - \frac{\sqrt{s}}{\gamma}Y'_o\right)^2 + \frac{s+1}{\gamma^2}X'^2_o\right]^{1/2}\right| + \sqrt{\frac{s}{s-1}}\left|\left[\left(Y_o - \frac{\sqrt{s}}{\gamma}X'_o\right)^2 + \frac{s-1}{\gamma^2}Y'^2_o\right]^{1/2}\right| \leq a \quad (11)$$

4. The Classical Channel

When the electric fields existing across the drift spaces between quadrupole sections are ignored the motions in the X-Z and Y-Z planes are uncoupled. Thus, particle motion in each of these planes may be considered separately. For such a structure, consisting of a cascade of symmetric triplets, it has been shown that motion through the i<u>th</u> triplet can be described by[4]

$$\begin{bmatrix} X_i \\ X'_i \end{bmatrix} = [C][d][D][D][d][C] \begin{bmatrix} X_{i_o} \\ X'_{i_o} \end{bmatrix} \quad (12)$$

$$\begin{bmatrix} Y_i \\ Y'_i \end{bmatrix} = [D][d][C][C][d][D] \begin{bmatrix} Y_{i_o} \\ Y'_{i_o} \end{bmatrix} \quad (13)$$

where

$$[C] = \begin{bmatrix} \cos\frac{\gamma\ell}{2} & (1/\gamma)\sin\frac{\gamma\ell}{2} \\ -\gamma\sin\frac{\gamma\ell}{2} & \cos\frac{\gamma\ell}{2} \end{bmatrix}$$

$$[D] = \begin{bmatrix} \cosh\frac{\gamma\ell}{2} & (1/\gamma)\sinh\frac{\gamma\ell}{2} \\ \gamma\sinh\frac{\gamma\ell}{2} & \cosh\frac{\gamma\ell}{2} \end{bmatrix}$$

$$[d] = \begin{bmatrix} 1 & d \\ 0 & 1 \end{bmatrix}$$

and where as previously defined $\gamma = \sqrt{V_o/V}/a$. X_{i_o}, Y_{i_o}, X'_{i_o} and Y'_{i_o} are values of the transverse displacements and normalized momenta of the particle at the entry of the i<u>th</u> triplet, while X_i, Y_i, X'_i and Y'_i are the conditions of the particle at the exit of the i<u>th</u> triplet. Conditions at the entry of this triplet are expressed in terms of X_o, Y_o, X'_o and Y'_o by successive matrix multiplications. The transverse displacement and momentum of a particle at some arbitrary distance along the triplet can be found by performing the matrix multiplications indicated by equations (12) and (13) one at a time until conditions at the entry of the appropriate section have been determined. Finally, the values of X, Y, X' and Y' at the desired position are evaluated using one of the transformations [C], [D] or [d] with $\ell/2$ or d replaced by the axial distance of the particle from the entrance of the section.

It can be shown from the work of Septier[4] that stable motion of particles along a cascade of such triplets will result if

$$-1 < [\cos\gamma\ell\cosh\gamma\ell + \gamma d\{\cos\gamma\ell\sinh\gamma\ell - \sin\gamma\ell\cosh\gamma\ell\} - (\gamma^2d^2/2)\sin\gamma\ell\sinh\gamma\ell] < 1 \quad (14)$$

When d = 0, equations (1) and (14) may be used to show that stable motion will result if

$$0 < L\sqrt{V_o/V}/4a < 1.873 \quad (15)$$

Equation (15) is analogous to equation (8) for the twisted structure.

In order that particles be confined within the structure it is necessary that the maximum displacement in the X and in the Y directions be less than or at most equal to the aperture radius. Thus, since motion in the X-Z and Y-Z planes is uncoupled, $X_{max} \leq a$ and $Y_{max} \leq a$. Smith et al.[5] have shown that these conditions will be satisfied for a long chain of triplets when

$$[X_o/a]^2 + [X'_o/\gamma_x a]^2 \leq 1 \quad (16)$$

and

$$[\psi Y_o/a]^2 + [Y'_o/\gamma_x\psi a]^2 \leq 1 \quad (17)$$

where it may be shown that

$$\gamma_x = \gamma\left[\frac{\{\sin\gamma\ell\cosh\gamma\ell - \sinh\gamma\ell\} + \gamma d\{\sin\gamma\ell\sinh\gamma\ell \ldots}{\{\sin\gamma\ell\cosh\gamma\ell + \sinh\gamma\ell\} + \gamma d\{\sin\gamma\ell\sinh\gamma\ell \ldots}\right.$$
$$\left.\frac{-(1-\cos\gamma\ell)\cosh\gamma\ell - \frac{\gamma^2d^2}{2}(1-\cos\gamma\ell)\sinh\gamma\ell}{+(1+\cos\gamma\ell)\cosh\gamma\ell + \frac{\gamma^2d^2}{2}(1+\cos\gamma\ell)\sinh\gamma\ell}\right]^{1/2}$$

and

$$\psi^2 = \frac{\cos\frac{\gamma\ell}{2}\cosh\frac{\gamma\ell}{2} + \sin\frac{\gamma\ell}{2}\sinh\frac{\gamma\ell}{2} + \gamma d\cos\frac{\gamma\ell}{2}\sinh\frac{\gamma\ell}{2}}{\cos\frac{\gamma\ell}{2}\cosh\frac{\gamma\ell}{2} - \sin\frac{\gamma\ell}{2}\sinh\frac{\gamma\ell}{2} - \gamma d\sin\frac{\gamma\ell}{2}\cosh\frac{\gamma\ell}{2}}$$

In contrast to the twisted structure, values of X_o and X'_o can be specified independently of values of Y_o and Y'_o.

5. Comparison of Acceptance Limits

The comparison will be restricted to the discussion of the special cases of injection parallel to the Z-axis, injection from a point source at Z = 0, injection in the X-Z plane with X-directed transverse momentum and injection in the Y-Z plane with Y-directed transverse momentum. In each case note that the quantity $(X_oY'_o - Y_oX'_o)$, equals zero, in which case $s = (2-/\gamma L)^2$. For the calculations to follow it will be assumed for both structures that $(2\pi a/L)^2 = 0.1$.

Injection in the X-Z Plane ($Y_o = Y'_o = 0$):

Substituting $Y_o = Y'_o = 0$ in equation (11) yields, after some manipulation,

$$\left[\frac{|X'_o| - \gamma a\, s\sqrt{s-1}}{\beta a\sqrt{s+1}\,(s-1)}\right]^2 - \left[\frac{X_o}{a\sqrt{s^2-1}}\right]^2 \leq 1$$

Equation (18) defines two intersecting hyperbolic curves. The region interior to these curves represents the acceptance area of the twisted structure in the phase plane $(X_o\text{-}X'_o)$. The maximum allowable values of $|X_o|$ and $|X'_o|$ are found to be

$$|X_o|_{max} = a \quad \text{when} \quad |X'_o| = 0$$

and $$|X'_o|_{max} = \beta a[s\sqrt{s-1} - \sqrt{s+1}(s-1)]/\sqrt{s} \quad \text{when} \quad |X_o| = 0.$$

For values of s approaching either 1 or infinity $|X'_o|_{max}$ approaches zero. For a structure of fixed a and L it is easily shown that $|X'_o|_{max}$ has a peak value when s = 1.3295. For a practical structure s can be varied simply by adjusting the quadrupole voltage, V_o.

For the classical channel the acceptance area is bounded by the elliptical curve defined by equation (16). Corresponding values of $|X_o|_{max}$ and $|X'_o|_{max}$ thus become:

$$|X_o|_{max} = a \quad \text{when} \quad X'_o = 0$$

$$|X'_o|_{max} = \gamma_x a \quad \text{when} \quad X_o = 0$$

The acceptance limits of the two structures in the $X_o\text{-}X'_o$ phase plane are compared in Fig. 3 for three different values of quadrupole voltage corresponding to s = 1.5, 2 and 3. Since the curves are symmetric only the first quadrant is shown. The classical structure has been assumed to have no drift spaces. Also shown in Fig. 3 is one additional curve representing the acceptance of a classical channel for which s = 2, that is, $\gamma L/4 = 1.11$, and $d/\ell = 0.25$. It is clear that, although the values of $|X_o|_{max}$ are identical, the acceptable maximum values of $|X'_o|$ are considerably larger for the twisted structure in every case. Moreover in practice, where a drift space must be introduced, the allowable value of $|X'_o|_{max}$ for the classical structure is further reduced.

Injection in the Y-Z Plane ($X_o = X'_o = 0$):

Substituting $X_o = X'_o = 0$ in equation (11) gives

$$\frac{s}{s-1}\frac{|Y_o|^2}{a^2} + \frac{2\sqrt{s}}{\gamma a}|Y'_o| \leq 1 \quad (19)$$

The area enclosed by these intersecting parabolic curves represents the acceptance area of the twisted structure in the $Y_o\text{-}Y'_o$ phase plane. The maximum allowable values of $|Y_o|$ and $|Y'_o|$ are found to be

$$|Y_o|_{max} = \sqrt{\frac{s-1}{s}}\,a \quad \text{when} \quad |Y_o| = 0$$

and $$|Y'_o|_{max} = \beta a/2s \quad \text{when} \quad |Y_o| = 0$$

As s approaches 1, $|Y'_o|_{max}$ approaches a maximum value of $\beta a/2$, but $|Y_o|_{max}$ goes to zero. On the other hand for large values of s, $|Y_o|_{max}$ approaches the aperture radius and $|Y'_o|_{max}$ approaches zero. The acceptance area reaches a maximum value when s = 1.5.

For the classical channel the acceptance area is bounded by the elliptical curve defined by equation (17). Corresponding values of $|Y_o|_{max}$ and $|Y'_o|_{max}$ then become

$$|Y_o|_{max} = a/\beta \quad \text{when} \quad |Y'_o|_{max} = 0$$

and $$|Y'_o|_{max} = \gamma_x\beta a \quad \text{when} \quad |Y_o| = 0$$

The acceptance in the $Y_o\text{-}Y'_o$ plane is compared for the two structures in Fig. 4. The acceptable maximum values of normalized transverse momentum at injection are significantly greater for the twisted structure. The relative magnitudes of $|Y_o|_{max}$ depend on the value of s and hence γL. For the case s = 3, the value of $|Y_o|_{max}$ for the twisted structure is marginally larger than the corresponding value for the classical channel. However for s = 1.5, and s = 2 the reverse is true. The introduction of a drift space can be seen to reduce $|Y'_o|_{max}$ while very slightly increasing $|Y_o|_{max}$ for the classical channel.

Injection Parallel to Z-Axis ($X'_o = Y'_o = 0$):

Setting the initial transverse momenta to zero in equation (11), gives,

$$\frac{|X_o|}{a} + \sqrt{\frac{s}{s-1}}\,\frac{|Y_o|}{a} \leq 1 \qquad (20)$$

The straight lines defined by equation (20) bound a parallelogram shaped area representing the acceptance of the twisted structure in the X-Y plane. In this case

$$|X_o|_{max} = a \quad \text{when } |Y_o| = 0$$

$$|Y_o|_{max} = \sqrt{\frac{s-1}{s}}\,a \quad \text{when } |X_o| = 0$$

The acceptance area of the classical structure is a rectangle bounded in the X-Y plane by the straight lines given by equations (16) and (17) with $X'_o = Y'_o = 0$. Hence,

$$|X_o|_{max} = a \quad , \quad |Y_o|_{max} = a/\psi$$

In Fig. 5 the twisted structure is compared to the classical channel with $d/\ell = 0$ and $d/\ell = 0.25$. The introduction of a drift space has increased $|Y_o|_{max}$ for the classical channel. Thus for the classical structure with or without drift spaces $|Y_o|_{max}$ is greater than the corresponding value for the twisted quadrupole. The uncoupled motion along the triplet chain has resulted in a significantly greater acceptance in the X-Y plane. However, in practice, it can be expected that the difference in the acceptances will be less because of the influence of the fringing fields existing between each and every section of the classical channel.

Injection From a Point Source at Z = 0 ($X_o = Y_o = 0$):

When the particle is injected into the twisted channel from a point on the axis at Z = 0, equation (11) becomes:

$$\left|[sY_o'^2+(s+1)X_o'^2]^{1/2}\right| + \sqrt{\frac{s}{s-1}}\;\left|[sX_o'^2+(s-1)Y_o'^2]^{1/2}\right| \leq \gamma a \qquad (21)$$

The acceptance area of the twisted structure in this case is bounded by an ellipsoidal-like curve with major and minor axes oriented in the X'_o and Y'_o directions. The maximum values of X'_o and Y'_o become

$$|X'_o|_{max} = \beta a[s\sqrt{s-1} - \sqrt{s+1}(s-1)]/\sqrt{s} \quad \text{when } |Y'_o| = 0$$

$$|Y'_o|_{max} = \beta a/2s \quad \text{when } |X'_o| = 0$$

As s approaches infinity both $|X'_o|_{max}$ and $|Y'_o|_{max}$ approach zero and the acceptance area is reduced to zero. Similarly as s approaches 1 the area goes to zero since $X'_o|_{max}$ approaches zero. The acceptances of the twisted and classical channels are compared in Fig. 6. From equations (16) and (17) with $X_o = Y_o = 0$, the acceptance area for the classical channel is seen to be a rectangle bounded by the straight lines

$$|X'_o|_{max} = \gamma_x a \quad , \quad |Y'_o|_{max} = \gamma_x \beta a$$

It is apparent that over much of the region the allowable values of $|X'_o|$ and $|Y'_o|$ are significantly greater for the twisted quadrupole than for the chain of triplets. Introduction of a drift space is seen to further reduce the acceptance of the classical channel.

In conclusion, the uniformly twisted quadrupole seems capable of handling more widely divergent particle beams than can the classical cascade of triplet sections. Further evidence of this strong focusing action can be obtained from the comparison of the trajectories of individual particles along the twisted and classical structure. Particles with a wide variety of injection conditions have been traced through both channels. In every case, for identical injection conditions, the projections of the particle's trajectory in the X-Z and Y-Z planes first cross the Z-axis in the twisted structure. A typical projection in the Y-Z plane is shown in Fig. 7 for a particle with $X_o = Y_o = X'_o = 0$ and $Y'_o = 0.07$. In this particular example s = 2.

6. Acknowledgement

The authors would like to express their thanks to the National Research Council of Canada for financial support of this work.

7. References

1. A.P. Banford, "The Transport of Charged Particle Beams", E. & F.N. Spon Limited, London, p. 100-119, 1966.
2. F.S. Chute, F.E. Vermeulen and E.A. Youssef, Nucl. Inst. Meth., Vol. 82, p. 86-92, 1970.
3. K. Ogatta, "State Space Analysis of Control Systems", Prentice Hall, p. 108, 1967.
4. A.L. Septier, "Advances in Electronics and Electron Physics", Vol. 14, p. 85-205, 1961.
5. L. Smith and R.L. Gluckstern, Rev. Sci. Instr., Vol. 26, No. 2, p. 220-228, 1955.

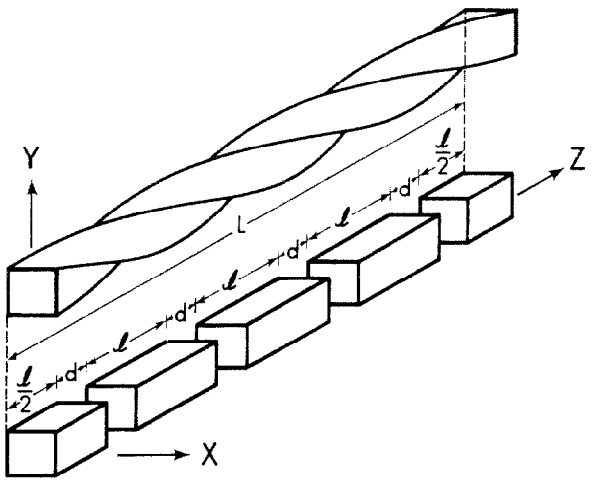

Fig. 2 A Schematic Representation of the Twisted and the Classical Structures to be Compared.

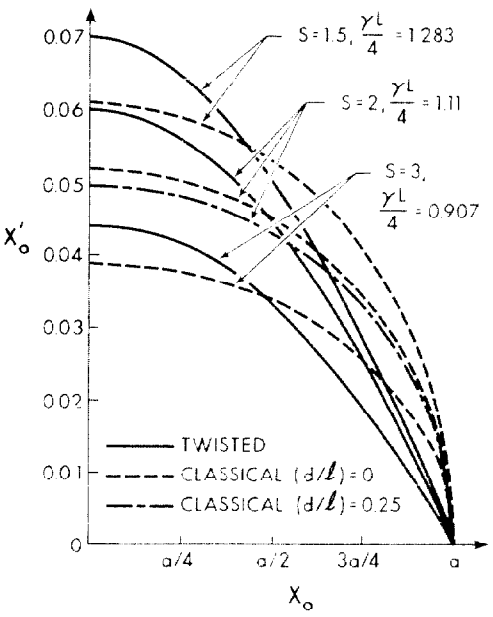

Fig. 3 Acceptance in the X_o - X'_o Plane.

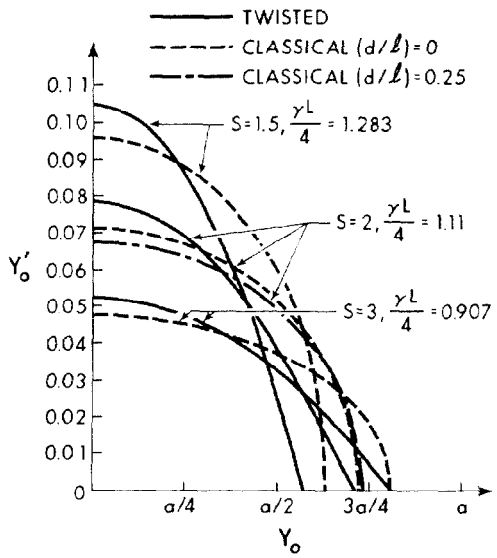

Fig. 4 Acceptance in the Y_o - Y'_o Plane.

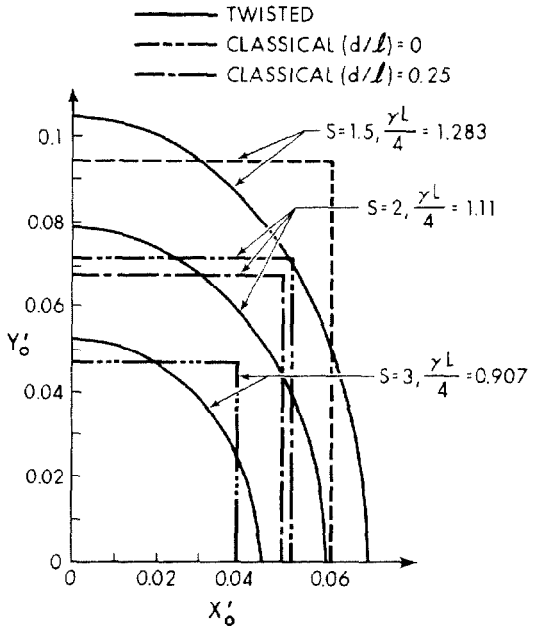

Fig. 6 Acceptance in the X'_o - Y'_o Plane.

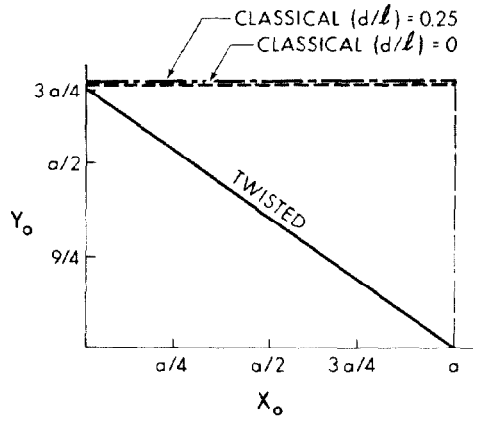

Fig. 5 Acceptance in the X_o - Y_o Plane.

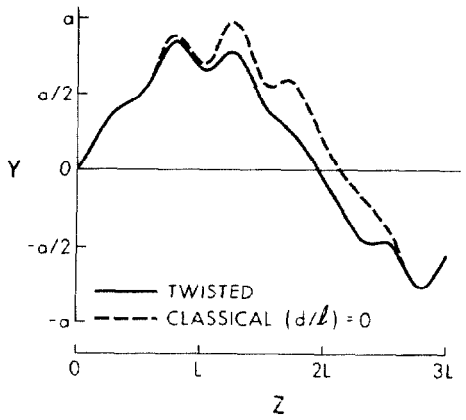

Fig. 7 The Y-Z Projection of a Typical Particle Trajectory.